

## Study of dimuon production in Indium-Indium collisions with the NA60 experiment

R. Shahoyan<sup>2,5</sup>, R. Arnaldi<sup>9</sup>, K. Banicz<sup>2,4</sup>, J. Castor<sup>3</sup>, B. Chaurand<sup>7</sup>, C. Cicalo<sup>1</sup>, A. Colla<sup>9</sup>,  
P. Cortese<sup>9</sup>, S. Damjanovic<sup>4</sup>, A. David<sup>2,5</sup>, A. de Falco<sup>1</sup>, A. Devaux<sup>3</sup>, L. Ducroux<sup>6</sup>, H. En'yo<sup>8</sup>,  
A. Ferretti<sup>9</sup>, M. Floris<sup>1</sup>, P. Force<sup>3</sup>, N. Guettet<sup>2,3</sup>, A. Guichard<sup>6</sup>, H. Gulkanian<sup>10</sup>, J. Heuser<sup>8</sup>, M. Keil<sup>2,4</sup>,  
L. Kluberg<sup>2,7</sup>, J. Lozano<sup>5</sup>, C. Lourenço<sup>2</sup>, F. Manso<sup>3</sup>, A. Masoni<sup>1</sup>, P. Martins<sup>2,5</sup>, A. Neves<sup>5</sup>, H. Ohnishi<sup>8</sup>,  
C. Oppedisano<sup>9</sup>, P. Parracho<sup>2</sup>, P. Pillot<sup>6</sup>, G. Puddu<sup>1</sup>, E. Radermacher<sup>2</sup>, P. Ramalhete<sup>2,5</sup>, P. Rosinsky<sup>2</sup>,  
E. Scomparin<sup>9</sup>, J. Seixas<sup>2,5</sup>, S. Serci<sup>1</sup>, P. Sonderegger<sup>5</sup>, H.J. Specht<sup>4</sup>, R. Tieulent<sup>6</sup>, G. Usai<sup>1</sup>,  
R. Veenhof<sup>2,5</sup> and H.K. Wöhri<sup>2,5</sup>

<sup>1</sup>*Univ. di Cagliari and INFN, Cagliari, Italy;* <sup>2</sup>*CERN, Geneva, Switzerland;* <sup>3</sup>*LPC, Univ. Blaise  
Pascal and CNRS-IN2P3, Clermont-Ferrand, France;* <sup>4</sup>*Univ. Heidelberg, Heidelberg, Germany;*

<sup>5</sup>*IST-CFTP, Lisbon, Portugal;* <sup>6</sup>*IPN-Lyon, Univ. Claude Bernard Lyon-I and CNRS-IN2P3, Lyon,  
France;* <sup>7</sup>*LLR, Ecole Polytechnique and CNRS-IN2P3, Palaiseau, France;* <sup>8</sup>*RIKEN, Wako, Saitama,  
Japan;* <sup>9</sup>*Univ. di Torino and INFN, Italy;* <sup>10</sup>*YerPhI, Yerevan, Armenia*

The NA60 experiment at the CERN-SPS is devoted to the study of dimuon production in heavy-ion and proton-nucleus collisions. We present preliminary results from the analysis of Indium-Indium collisions at 158 GeV per nucleon. The topics covered are low mass vector meson production,  $J/\psi$  production and suppression, and the feasibility of the open charm measurement from the dimuon continuum in the mass range below the  $J/\psi$  peak.

The study of dimuon production in heavy-ion collisions is generally considered to be one of the most powerful tools in the search for the phase transition between the normal nuclear matter and the Quark-Gluon Plasma phase, where the quarks and gluons are no longer confined into hadrons. The most intriguing findings of dilepton experiments working in this field have been: the excess in the production of dielectron pairs in the mass window 200–700 MeV/ $c^2$ , together with the flattening of the  $\rho$  and  $\omega$  peaks, observed by the NA45/CERES experiment in S-Au and Pb-Au collisions<sup>1</sup>; the anomalous  $J/\psi$  suppression found by NA50 in central Pb-Pb collisions<sup>2</sup>; and the excess in the production of dimuons in the “intermediate mass region”, 1.2–2.7 GeV/ $c^2$ , seen by NA38 and NA50 in S-U and Pb-Pb collisions<sup>3</sup>, and by HELIOS-3 in S-W collisions<sup>4</sup>. This paper presents the analysis of these topics using  $\sim 230$  million Indium-Indium dimuon events collected by NA60 in 2003.

The NA60 apparatus complements a Muon Spectrometer and a Zero Degree Calorimeter with a Vertex Telescope<sup>5</sup> made of Silicon pixel planes embedded in a 2.5 T dipole field and a Beam Tracker measuring the transverse coordinates of the incoming ion before its interaction in the target. The Vertex Telescope allows us to reconstruct the interaction vertex. Figure 1 shows the dispersion between the transverse position of the fitted vertex and of the Beam Tracker prediction, as a function of the number of tracks associated with the vertex. The corresponding vertex resolution is also shown. For most of our data it is better than 10  $\mu\text{m}$  in  $X$  (bending plane) and better than 15  $\mu\text{m}$  in  $Y$ .

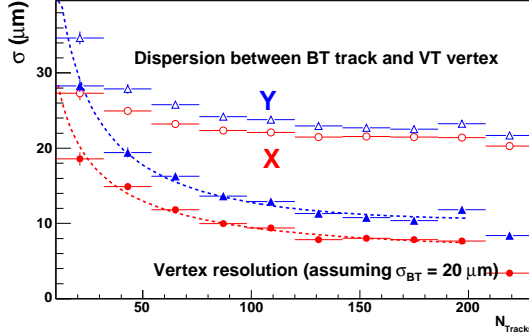


Figure 1: Dispersion between the fitted vertex and the Beam Tracker prediction (open symbols) and extracted vertex resolution (closed symbols), assuming a Beam Tracker precision of  $20 \mu\text{m}$ .

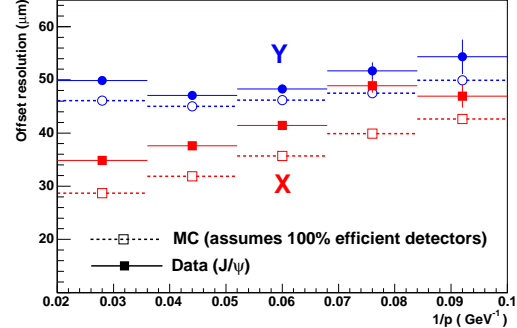


Figure 2: Measured offset resolution for  $\text{J}/\psi$  muons (solid symbols) compared to the resolution expected from a Monte Carlo simulation, assuming fully efficient pixel planes (open symbols).

The essential feature of NA60 is the matching between the muons reconstructed in the Muon Spectrometer and the tracks measured in the Vertex Telescope before they scatter in the hadron absorber. This improves the mass resolution from  $\sim 75 \text{ MeV}/c^2$  to  $\sim 20 \text{ MeV}/c^2$ , at the  $\omega$  mass. Additionally, the measurement of the impact parameter (offset) of the muons at the production vertex allows us to tag the muons from open charm decays. Figure 2 shows the offset resolution measured for  $\text{J}/\psi$  muons, which are expected to come exactly from the interaction point, as a function of their inverse momentum. Expected values from Monte Carlo simulations are also shown. In order to take into account the dependence of the muon offset resolution on its momentum, the measured offsets are weighted by the inverse of their covariant error matrices,  $V^{-1}$ , which incorporate the uncertainties from the vertex fit and from the muon extrapolation,  $\Delta = \sqrt{\Delta x^2 V_{xx}^{-1} + \Delta y^2 V_{yy}^{-1} + 2\Delta x \Delta y V_{xy}^{-1}}$ . Another benefit of the matching procedure is a strong reduction of the combinatorial background from uncorrelated  $\pi$  and  $\text{K}$  decays.

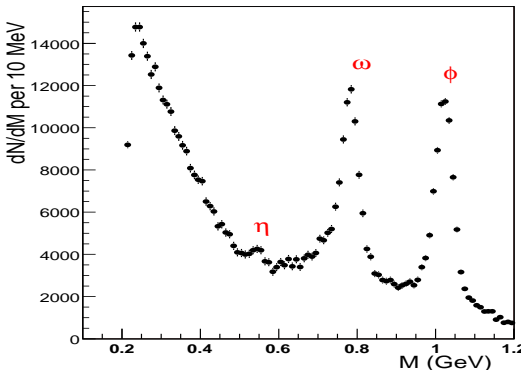


Figure 3: Dimuon mass distribution in In-In collisions, after background subtraction.

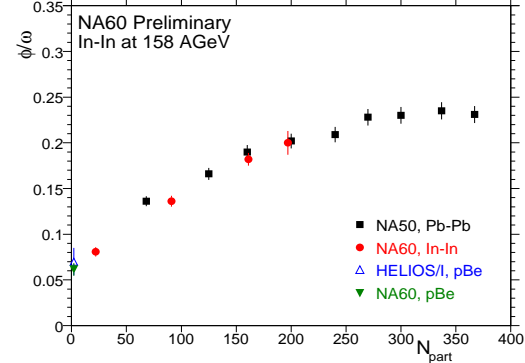


Figure 4: The  $\phi/\omega$  cross section ratio as a function of the number of participants.

Figure 3 shows the dimuon mass distribution measured in In-In collisions, after combinatorial background subtraction, integrating all collision centralities. The mass resolution is 23 MeV at the  $\phi$ . The extracted  $\phi/\omega$  values are shown in Fig. 4, in four centrality bins, as a function of the number of participants evaluated from a Glauber fit to the energy spectrum measured by the ZDC. The figure includes values obtained from the NA50 measurements in Pb-Pb collisions<sup>6</sup>. We have assumed that the  $\rho$  and  $\omega$  production cross sections are identical. In order to have both data sets reported in the same phase space region, we converted the NA50 points from the window  $m_T > 1.5 \text{ GeV}$  to the window  $p_T > 1.1 \text{ GeV}/c$ , using the inverse slope parameter measured by NA50,  $T = 228 \text{ MeV}$ , for the extrapolation<sup>7</sup>. The Pb-Pb and In-In values are

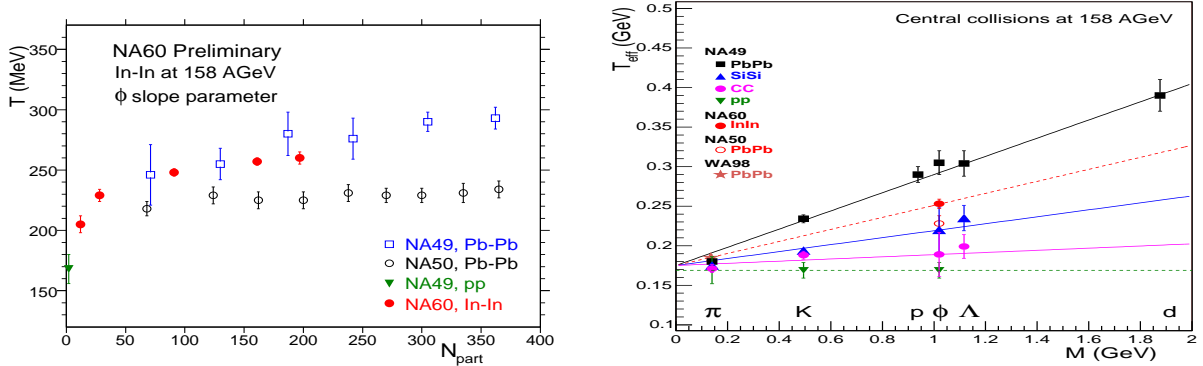


Figure 5: The  $\phi$   $m_T$  inverse slope parameter,  $T$ , as a function of the number of participants (left) and of the particle mass and colliding system (right).

in good agreement, suggesting that  $N_{\text{part}}$  is a good scaling variable to describe the  $\phi/\omega$  ratio. We have studied the  $\phi$  transverse momentum distribution, selecting signal dimuons in a narrow window at the  $\phi$  mass. Thanks to the presence of the dipole field in the vertex region we have a good dimuon acceptance down to zero  $p_T$ . Figure 5-left shows how the  $m_T$  inverse slopes extracted from our data compare with the Pb-Pb values measured by NA50<sup>6</sup> and NA49<sup>8</sup>, as a function of the number of participants. There is a clear increase of  $T$  between peripheral and central In-In collisions, from  $\sim 218$  MeV to  $\sim 255$  MeV, with  $T = 252 \pm 3$  MeV when integrating over all collision centralities. Figure 5-right compares our extracted  $\phi$  temperature with the measurements of other experiments as a function of the particle mass and colliding system.

We tag the dimuons as being “displaced” if both muons have weighted offsets above 1 (roughly 90  $\mu\text{m}$  for muons with momenta around 15  $\text{GeV}/c$ ), otherwise they are tagged as “prompt”. To reject events where the interaction vertex was misidentified, this selection is only validated if the weighted transverse distance between the two muons, at the  $Z$  of the interaction vertex, is more than 0.7 for the “displaced” events and less than 2 for the “prompt” ones. The mass spectra for the two event samples are shown in Fig. 6. The regions dominated by the  $\omega$ ,  $\phi$  and  $J/\psi$  peaks are strongly suppressed in the displaced sample, as is clearly shown in the ratio between displaced and prompt mass spectra.

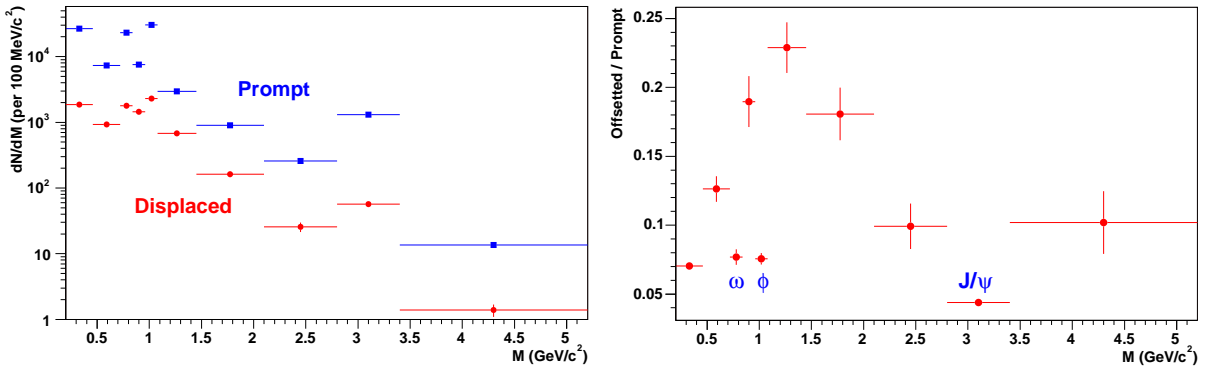


Figure 6: Dimuon mass spectra from the “displaced” and “prompt” samples (left), and their ratio (right).

Among the interesting observations made by previous experiments studying high-energy heavy-ion physics at the CERN SPS stands the observation, by NA50, that the production yield of  $J/\psi$  mesons is suppressed in central Pb-Pb collisions beyond the normal nuclear absorption defined by proton-nucleus data. This behaviour is expected to occur if the matter produced in these extreme collisions goes through a phase of deconfined partonic matter, where the charmonium states should be dissolved when critical thresholds are exceeded, either in the medium temperature (thermal transition, QGP) or in the density of interacting partons (geometrical

transition, percolation). By comparing the centrality dependence of the suppression pattern between two different colliding systems, Pb-Pb and In-In, we should be able to identify the corresponding scaling variable and the physics mechanism driving the suppression.

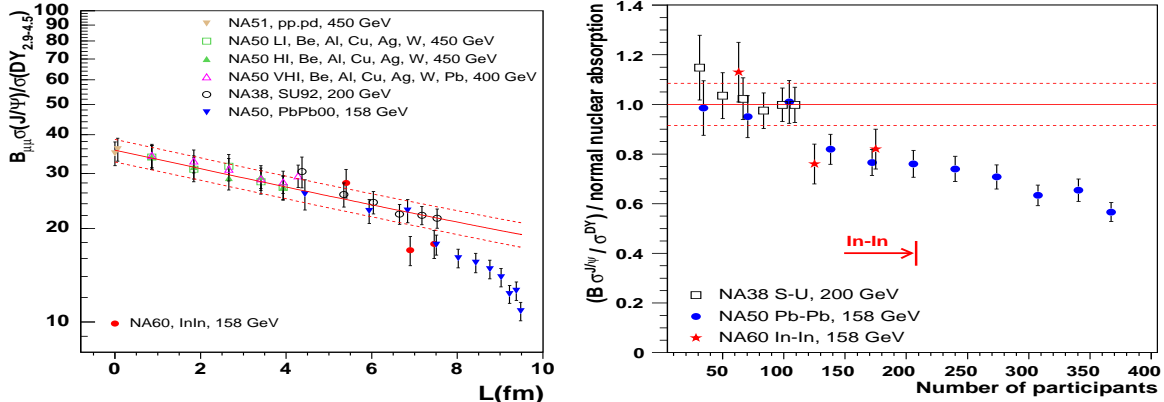


Figure 7:  $\text{J}/\psi$  suppression before (left, versus  $L$ ) and after (right, versus  $N_{\text{part}}$ ) dividing by the normal nuclear absorption curve.

Figure 7 shows the ratio between the  $\text{J}/\psi$  and the Drell-Yan production cross-sections measured in In-In collisions, in three centrality bins, either as a function of  $L$  (the distance of nuclear matter crossed by the  $\text{J}/\psi$  mesons after production) or  $N_{\text{part}}$ . On the right panel the  $\text{J}/\psi$  suppression pattern is divided by the normal nuclear absorption curve, defined by p-nucleus data<sup>9</sup>. The  $\text{J}/\psi$  and Drell-Yan cross-sections are evaluated in the phase space window  $2.92 < y_{\text{lab}} < 3.92$  and  $-0.5 < \cos \theta_{\text{CS}} < 0.5$ , where  $\theta_{\text{CS}}$  is the polar decay angle of the muons in the Collins-Soper reference system. The Drell-Yan value is given in the  $2.9\text{--}4.5 \text{ GeV}/c^2$  mass window. We see that, unlike what happens in the S-U collisions studied by NA38, the  $\text{J}/\psi$  production is suppressed in indium-indium collisions beyond the normal nuclear absorption. When the  $\text{J}/\psi$  over Drell-Yan ratio is plotted as a function of  $N_{\text{part}}$  the indium data points are in good agreement with the suppression pattern measured in Pb-Pb. The two sets of data points *do not* overlap as a function of  $L$ . We are presently studying the  $\text{J}/\psi$  suppression pattern without making the ratio with respect to the Drell-Yan yield, so that we can have more centrality bins, and as a function of the energy density, to clarify the origin of the anomalous  $\text{J}/\psi$  suppression.

We are also analysing the proton-nucleus data collected in 2004, with 158 GeV protons colliding on 7 different nuclear targets, to determine the normal nuclear absorption of the  $\text{J}/\psi$  in the energy and kinematical domains of the heavy-ion data, without the model dependent assumptions presently used to correct the NA50 proton data, collected at 400 or 450 GeV.

This work was partially supported by the Fundação para a Ciência e a Tecnologia, Portugal.

1. G. Agakichiev *et al.* (CERES Coll.), Phys. Rev. Lett. **75**, (1995) 1272; Phys. Lett. **B422** (1998) 405; B. Lenkeit *et al.* (CERES Coll.), Nucl. Phys. **A661**, (1999) 23c.
2. B. Alessandro *et al.* (NA50 Coll.), Eur. Phys. J. **C39** (2005) 335; A. Baldit *et al.* (NA50 Coll.), Phys. Lett. **B140** (1997) 337.
3. M.C. Abreu *et al.* (NA50 Coll.), Eur. Phys. J. **C14** (2000) 443.
4. A.L.S. Angelis *et al.* (HELIOS-3 Coll.), Eur. Phys. J. **C13** (2000) 433.
5. K. Banicz *et al.*, Nucl. Instrum. Meth. **A539** (2005) 137.
6. D. Jouan *et al.* (NA50 Coll.), J. Phys. **G30** (2004) S277; B. Alessandro *et al.* (NA50 Coll.), Phys. Lett. **B 555** (2003) 147.
7. G. Usai *et al.* (NA60 Coll.), Proc. of Hard Probes 2004, Eur. Phys. J. **C**.
8. V. Friese *et al.* (NA49 Coll.), Nucl. Phys. **A698** (2002) 487c.
9. G. Borges *et al.* (NA50 Coll.), these proceedings.